Journal of Engineering Science and Technology
Vol. 9, No. 4 (2014) 423 - 431

DESIGN OF BACKWARD SWEPT TURBINE WHEEL FOR CRYOGENIC TURBOEXPANDER

BALAJI K. CHOUDHURY*, RANJIT K. SAHOO, SUNIL K. SARANGI

Department of Mechanical Engineering, NIT Rourkela-769008, Odisha, India
*Corresponding Author: balajichoudhury@gmail.com

Abstract

With support from the Department of Atomic Energy, our institute has initiated a programme on development and study of a low capacity (20 liters/hr.) turboexpander based Nitrogen liquefier. Hence a process design was carried out and a turboexpander was designed to meet the requirement of the liquefier. The turboexpander is used for lowering the temperature of the process gas (Nitrogen) by the isenthalpic expansion. The efficiency of the turboexpander mainly depends on the specific speed and specific diameter of the turbine wheel. The paper explains a general methodology for the design of any type of turbine wheel (radial, backward swept and forward swept) for any pressure ratio with different process gases. The design of turbine wheel includes the determination of dimensions, blade profile and velocity triangles at inlet and outlet of the turbine wheel. Generally radial turbine wheels are used but in this case to achieve the high efficiency at desired speed, backward curved blades are used to maintain the Mach number of the process gas at the nozzle exit, close to unity. If the velocity of fluid exceeds the speed of sound, the flow gets choked leading to the creation of shock waves and flow at the exit of the nozzle will be non-isentropic.

Keywords: Turboexpander, Turbine wheel, Backward swept blade.

1. Introduction

The performance of all cryogenic refrigeration and liquefaction plants mainly depends on the efficiency of turboexpander. The turboexpander is an expansion device where the process gas is expanded by lowering its temperature at turbine side and simultaneously rejecting heat at the brake compressor side. Hence the dimension of turbine and its blade profile plays a vital role in expanding the process gas and lowering the temperature of the gas. The turboexpander consists

Nomenclatures

b	Height (nozzle, impeller blade), m
C	Absolute velocity of fluid stream, m/s
C_o	Spouting velocity, m/s
C_s	Velocity of sound, m/s
D	Diameter, m
d_s	Specific diameter, dimensionless
h	Enthalpy, kJ/kg
k_1	Pressure recovery factor
k_2	Temperature and density recovery factor
M	Mach number
$\dot{m}$	Mass of nitrogen flow through turboexpander, kg/s
N	Rotational speed, rpm
n_s	Specific speed
P	Power output of the turbine, W
p	Pressure, N/m^2
Q	Volumetric flow rate, m^3/s
s	Specific entropy, kJ/kg K
T	Temperature, K
t	Blade thickness, m
U	Blade velocity (in tangential direction), m/s
Z	Number of blades

Greek Symbols

α	Absolute velocity angle, radian
α_0	Inlet flow angle, radian
α_t	Throat angle, radian
α_{tr}	Mass fraction of nitrogen diverted through turboexpander
β	Relative velocity angle, radian
η	Isentropic efficiency
λ_{tr}	Hub diameter to tip diameter ratio
ρ	Density, kg/m^3
ξ	Inlet turbine impeller diameter to exit tip diameter ratio
ω	Rotational speed, rad/s

Subscripts

o	Stagnation condition
hub	Hub of turbine impeller at exit
m	Meridional direction
max	Maximum
mean	Average of tip and hub
min	Minimum
r	Radial direction
s	Isentropic
t	Throat
tip	Tip of turbine impeller at exit
θ	Tangential direction

of a turbine impeller and a brake compressor at the two ends of a vertically placed shaft. The shaft is supported by two number of tilting pad journal bearing and two number of aerostatic thrust bearing. The whole components are place inside a bearing housing. At the lower end of bearing housing, cold end housing is attached. The cold end housing consists of nozzles and diffuser. At the top of bearing housing, warm end housing present. It consists of nozzle to the brake compressor. The sectional view of the turboexpander is shown in Fig. 1 and the design input parameters are shown in Table 1.

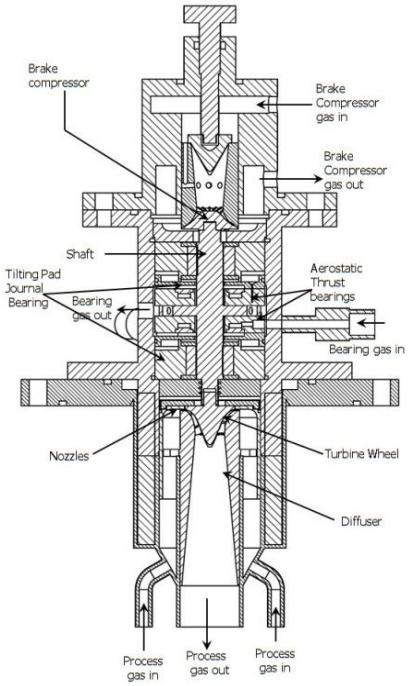

Fig. 1. Sectional View of Turboexpander Assembly.

Table 1. Design Input Parameters.

Working fluid	Nitrogen
Turbine inlet temperature, T_{in}	124 K
Turbine inlet pressure, p_{in}	7.97 bar
Discharge pressure, p_{ex}	1.2 bar
Mass flow rate, $\dot{m}$	76.46 kg/s

Working of Turboexpander

The process gas enters from the bottom end and gets expanded by passing through the nozzles and turbine impeller and comes out from the diffuser. The states points at nozzles, turbine impeller and diffuser are shown in Fig. 2. Due to the

isenthalpic expansion of the process gas the temperature decreases along with the pressure. Pressure recovery occurs due to the presence of diffuser. The *T-s* diagram of the turboexpander expansion process is shown in Fig. 3.

The design of turboexpander needs a fixed state of process stream parameters or design point. The design point is fixed as per the process design done for turboexpander based Nitrogen liquefier [1]. The literatures of design methods for turboexpander [2-5] are available for low expansion ratio with purely radial turbines. But the required design point have high expansion ratio (i.e., 6.64). The high expansion ratio is achieved by using backward curved vanes [6] which increase the tangential force on the blades thereby increasing the turbine speed for higher efficiency. The present design procedure has following characteristics:

- Design for any expansion ratio.
- Design of radial, backward or forward turbine.

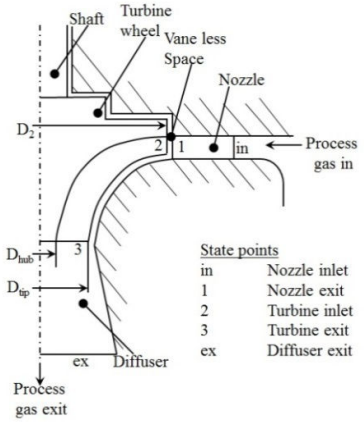

Fig. 2. State Points at Nozzles, Turbine Impeller and Diffuser.

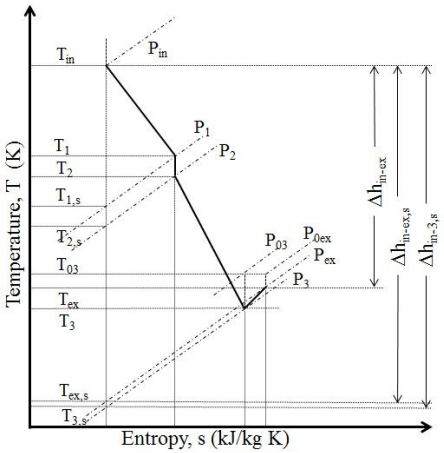

Fig. 3. *T-s* Diagram of Turboexpander.

2. Design of Turbine Wheel

The major dimensions of the turbine wheel and its inlet and exit velocity triangles are uniquely determined by the two dimensionless parameters [7], i.e., specific speed and specific diameter. The specific speed and specific diameter are expressed by the following equations

Specific speed,

$$n_s = \frac{\omega\sqrt{Q_3}}{\left(\Delta h_{in-3,s}\right)^{3/4}} \tag{1}$$

Specific diameter,

$$d_s = \frac{D_2\left(\Delta h_{in-3,s}\right)^{1/4}}{\sqrt{Q_3}} \tag{2}$$

where Q_3 is the volumetric flow rate at the exit of the turbine impeller and $\Delta h_{in\text{-}3,s}$ is the isentropic enthalpy drop from inlet to the turbine exit. The values of specific speed and specific diameter are chosen so that Mach number of the fluid at the nozzle exit is maintained at or close to unity. If the velocity of fluid exceeds the speed of sound, the flow gets choked leading to the creation of shock waves and flow at the exit of the nozzle will be non-isentropic. To achieve the maximum possible efficiency within the subsonic zone the specific speed and specific diameter are chosen so as 0.5471 and 3.4728 respectively. At known inlet input pressure and temperature all the rest thermodynamic properties can be calculated using property package ALLPROPS [8].

Considering reasonable turboexpander efficiency of 75%, enthalpy at exit, h_{ex} is calculated by following equation,

$$h_{ex} = h_{in} - \eta(h_{in} - h_{ex,s}) \tag{3}$$

Power produced,

$$P = \dot{m}\left(h_{in} - h_{ex}\right) \tag{4}$$

and volume flow rates at diffuser exit,

$$Q_{ex} = \dot{m} / \rho_{ex} \tag{5}$$

The states at the inlet and exit of the turboexpander are known. But states at turbine exit are not known. There is the difference between the states '3' and 'ex' caused by pressure recovery and consequent rise in temperature and density in the diffuser. The two factors k_1 and k_2 are taken in account, where

$$k_1 = Q_3 / Q_{ex} \tag{6}$$

and

$$k_2 = (h_{in} - h_{3s}) / h_{in} - h_{ex,s} \tag{7}$$

The value of k_1 is assumed to be 1.11 as taken by Ghosh [2] and k_2 value is taken as 1.03 from the suggestion of Kun and Sentz [5]. Substituting the values of

k_1 and k_2 in Eqs. (6) and (7) respectively we get, isentropic enthalpy drop from turbine $\Delta h_{in-3,s}$ and volumetric flow rate at exit of turbine impeller Q_3. Putting the values of $\Delta h_{in-3,s}$ and Q_3 into Eqs. (1) and (2) gives the speed and diameter of the turbine. The velocity ratio is calculated from the ratio of blade velocity to spouting velocity, where spouting velocity,

$$C_o = \sqrt{2(h_1 - h_{ex,s})} \tag{8}$$

As all radial turbines are found to produce maximum efficiencies over the range of velocity ratio 0.65 to 0.70 [9], the current design is limit to within limiting value. Rohlik [10] prescribes that; ξ the ratio of eye tip diameter to inlet diameter should be limited to a maximum value of 0.7 to avoid excessive shroud curvature. The value of ξ is taken as 0.6, corresponding to the maximum efficiency within the subsonic zone and for obtaining longer blade passages. Again from Reference [10], the exit hub to tip diameter ratio should be limited to a minimum value of 0.4 to avoid excessive hub blade blockage and energy loss. Kun and Sentz [5] have taken the ratio as 0.35 while Ino et al. [6] have chosen a value of 0.588. For current design the value of λ is taken as 0.425. Table 2 gives the estimated values of turbine impeller.

Table 2. Estimated Values of Turbine Impeller.

Inlet diameter	29.6 mm
Rotational speed	138777 rpm
Eye tip diameter	17.8 mm
Hub diameter	8.9 mm
Power output	2852.3 W
Velocity ratio	0.682

2.1. Turbine exit velocities

For small turbines, the number of blades depends on the hub circumference at exit and availability of diameter of milling cutters. So number of blades is taken $Z = 10$ [2]. Considering uniform thickness of blades is 0.6 mm [2]. Assuming absolute meridian velocity, C_{m3} and exit angle, α_3 as 95° [6] other velocity components are calculated along with mean blade angle at exit using following equations.

Absolute velocity at turbine exit,

$$C_3 = \frac{C_{m3}}{\sin \alpha_3} \tag{9}$$

Absolute tangential component,

$$C_{\theta 3} = C_3 \cos(\alpha_3) \tag{10}$$

Relative velocity at turbine exit,

$$W_3 = \sqrt{C_3^2 + U_3^2 - 2C_3U_3 \cos(\alpha_3)} \tag{11}$$

$$\beta_{3,mean} = \tan^{-1} \frac{C_3 \sin(\alpha_3)}{U_{3,mean} - C_3 \cos(\alpha_3)} \tag{12}$$

Flow through turbine

$$Q_3 = C_3 \sin(\alpha_3) \left[\frac{\pi}{4} \left({D_{3,tip}}^2 - {D_{3,hub}}^2 \right) - \frac{Zt_{tr} \left(D_{3,tip} - D_{3,hub} \right)}{2 \sin \beta_{3,mean}} \right] \tag{13}$$

Comparing the value of Q_3 in Eq. **Error! Reference source not found.** with the previously calculated value from Eq. (5), if they are not equal then change the value of C_{m3} until both the values are equal.

2.2. Turbine inlet velocities

Assume incidence angle, α_2 as 26^o [3]. The amount of work can be extracted from a turbine is calculated from change in momentum of the fluid in its passage through the turbine impeller. So simplifying the energy conservation equation for turbo machine [9], absolute velocity is calculated as

$$C_2 = \frac{1000(h_{02} - h_{03}) + U_3 C_3 \cos(\alpha_3)}{U_2 \cos(\alpha_2)} \tag{14}$$

And rest of the velocities estimated as follows.

$$C_{\theta 2} = C_2 \cos(\alpha_2) \tag{15}$$

$$C_{m2} = C_2 \sin(\alpha_2) \tag{16}$$

$$W_2 = \sqrt{{C_{m2}}^2 + (U_2 - C_{\theta 2})^2} \tag{17}$$

$$\beta_2 = \tan^{-1} \frac{C_{m2}}{(U_2 - C_{g2})} \tag{18}$$

It can be seen from Fig. 4 that the turbine impeller has backward swept blades. The blade profile has been worked out using the technique of Hasselgruber [11], which has been modified for the backward curved vanes.

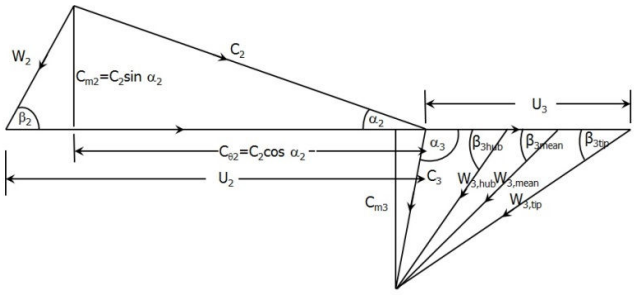

Fig. 4. Velocity Triangle at Inlet ant Exit of the Turbine Impeller.

Figure 5 shows the different types blade profile. In backward curved blades, the blades are inclined away from the direction of motion $\left(u_2 > C_2 \cos\alpha_2\right)$ give a higher value of blade velocity, u_2 for the given spouting velocity, C_0 and nozzle angle. Or, in other words, the same blade velocity gives a lower value of jet velocity compared to other type of blades. This permits more pressure drop in the nozzle, thus permitting the use of high expansion ratio within the subsonic zone.

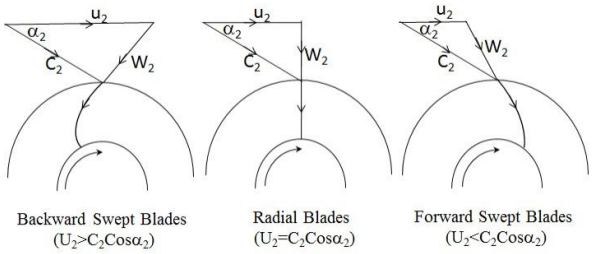

Fig. 5. Different Types of Blade.

2.3. Thermodynamic state at discharge (state at 3)

Neglecting losses in the diffuser, Stagnation enthalpy at turbine exit, h_{03} is equal to Stagnation enthalpy at diffuser exit h_{04}. From the stagnation enthalpy at turbine exit, static enthalpy at turbine exit is calculated. The density was found out by knowing the values of mass flow and volume flow at turbine exit by following equation

$$\rho_3 = \dot{m} / Q_3 \tag{19}$$

From h_3 and ρ_3, all the other properties at the turbine outlet are calculated from fluid property calculation software ALLPROPS [8].

2.4. Thermodynamic state at inlet (state at 2)

For computing the thermodynamic properties at impeller inlet (state 2), the efficiency of the expansion process till state 2 is assumed. Assuming isentropic expansion in the vane less space, the efficiency of the nozzle along with the vane less space is defined as

$$\eta_n = \frac{h_{in} - h_2}{h_{in} - h_{2s}} \tag{20}$$

From Eq. (20), taking the nozzle efficiency η_n as 93% [5, 6, and 12], the isentropic enthalpy at turbine inlet is calculated. Also due to isentropic at inlet to nozzle is equal to inlet to turbine, i.e., $s_{in} = s_1 = s_{2s}$. Knowing h_{2s} and s_{2s}, the other properties at turbine inlet are calculated along with the velocity of sound. Then absolute Mach number at the exit from the nozzle or inlet to the turbine impeller is calculated from the following equation which is to be less than 1 (i.e., 0.9388)

$$M = C_2 / C_{s2} \tag{21}$$

From continuity equation, the blade height at entrance to the impeller is computed from Eq. (22) as 0.709 mm.

$$b_2 = \frac{\dot{m}}{(\pi D_2 - Z_{tr} t_{tr}) \rho_2 C_{m2}} \tag{22}$$

3. Conclusions

The requirement of turboexpander to operate at high pressure ratios and with high velocities for better efficiency a backward curved turbine impeller is designed. It maintains the Mach number at inlet to the turbine and takes care of the velocity ratio (i.e., ratio of blade velocity to the spouting velocity) which is about 0.68.

References

1. Alur, S.A.; Choudhury, B.K.; Sahoo, R.K.; and Sarangi, S.K. (2010). Simulation of turboexpander based nitrogen liquefier. *Proceedings of the 20th National and 9th International ISHMT-ASME Heat and Mass Transfer Conference*, January 4-6, Mumbai, India.
2. Ghosh, P. (2002). *Analytical and experimental studies on cryogenic turboexpander*. Ph.D. Thesis, Indian Institute of Technology Kharagpur, India.
3. Ghosh, S.K. (2008). *Experimental and computational studies on cryogenic turboexpander*. Ph.D. Thesis. National Institute of Technology Rourkela, India.
4. Kun, L.C. (1988). Expansion turbines and refrigeration for gas separation and liquefaction. *Advances in Cryogenic Engineering*, 33, 963-973.
5. Kun, L.C.; and Sentz, R.N. (1985). High efficiency expansion turbines in air separation and liquefaction plants. *Proc. International Conference on Production and Purification of Coal Gas & Separation of Air*, 1-21.
6. Ino, N.; Machida, A.; Ttsugawa, K.; and Arai, Y. (1992). Development of high expansion ratio Helium turbo expander. *Advances in Cryogenic Engineering*, 37B, 835-844.
7. Balje, O.E. (1981). *Turbomachines*. John Wiley and Sons.
8. Lemmon, E.W.; Jacobsen, R.T.; Penoncello, S.G.; and Beyerlein, S.W. (1995). ALLPROPS 4.2 – Computer programs for calculating thermodynamic properties of fluids of engineering interest. *Centre for Applied Thermodynamic Studies, University of Idaho*.
9. Blackford, J.E.; Halford P.; and Tantam, D.H. (1971). Expander and pumps in G.G. Haselden (Ed.) *Cryogenic Fundamentals.* Academic Press London, 403-449.
10. RohliK, H.E. (1968). Analytical determination of radial inflow turbine geometry for maximum efficiency. *NASA TN D-4384*.
11. Hasselgruber, H. (1958). Stromungsgerechte gestaltung der laufrader von radialkompressoren mit axialem laufradeintrict Konstruction (in German). 10(1), 1-22.
12. Sixsmith, H.; and Swift W.L. (1986). *Cryogenic turbines and pumps in Hands*. Cryogenic Engineering Academic Press, 341-352.